ChemPubSoc Europe

DOI: 10.1002/chem.201501560

CHEMISTRY
A European Journal
Full Paper

Drug Delivery

Drug Release Properties of a Series of Adenine-Based Metal–Organic Frameworks

Hyojae Oh,[a] Tao Li,[b] and Jihyun An*[a]

Abstract: The drug uptake and release properties of a series of biomolecule-based metal–organic frameworks (bMOF-1, bMOF-4, bMOF-100, and bMOF-102) have been studied. The bMOFs were loaded with the small molecule etilefrine hydrochloride and release profiles were collected in both Nanopure water and simulated body fluid (SBF). Each bMOF exhibited an initial burst of drug release at the initial stages of the experiment followed by a gradual release of the remaining drug molecules over time. bMOF-1 released 50% of the drug after 15 days and complete release at 80 days in SBF. bMOF-4 released 50% of the drug within two days and complete release at 49 days in SBF. bMOF-100 and bMOF-102 released 50% of the drug after 4 h and complete release at 69 and 54 days in SBF, respectively.

Introduction

Among the numerous proposed applications for MOFs,[1,2] it has been suggested that MOFs might serve as a method for the introduction of therapeutic molecules into the body.[3] In particular, MOFs composed of nontoxic components are important for this application. Bio-MOFs (or bMOFs), which are defined as MOFs containing at least one biomolecular building block, have been constructed by using amino acids and nucleobases, for instance.[4–6] MOFs constructed from biomolecular building blocks are attractive for biological applications.[7,8] Drug delivery systems are of the utmost importance in treatment and medical research.[9,10] Maintaining the optimum concentration of drugs in the body is imperative to avoid side effects and maximize the effect of the drug. The ability to control drug release rates precisely over prolonged times in drug delivery systems has been highly anticipated.[11,12] MOFs have been explored extensively as candidate materials for drug delivery because of their highly tunable ordered structures and porosity.[13–21] Most of the MOFs studied for drug delivery have shown burst release of the guest drug molecules over a relatively short time period.[22–25] It has typically been quite difficult to control the rate of release of drug molecules incorporated into MOFs.

In this study, the drug loading and release properties of four different anionic adenine-based bMOFs are examined. Drug-release profiles in Nanopure water and simulated body fluid (SBF) are reported. bMOF degradation is closely monitored during the experiments to gain insight into the mechanism of the drug release process.

bMOF-1,[7] bMOF-4, bMOF-100,[5] and bMOF-102[26] were selected for this study. These materials are composed of a zinc-adeninate secondary building unit and a dicarboxylate organic ligand (biphenyl-4,4′-dicarboxylic acid (BPDC) for bMOF-1 and bMOF-100, and azobenzene-4,4′-dicarboxylic acid (Azo-BPDC) for bMOF-4 and bMOF-102). bMOF-1 and bMOF-4 have identical 1D porous structures, but have slightly different pore diameters, which are approximately 0.83 and 0.89 nm, respectively. Likewise, bMOF-100 and bMOF-102 also share the same 3D porous structure as each other and employ the same two ligands used in bMOF-1 and bMOF-4; their pore diameters are approximately 2.4 and 2.6 nm, respectively (Figure 1 A–D). These negatively charged frameworks were chosen to maximize the potential to strongly attract positively charged molecules into the pore.

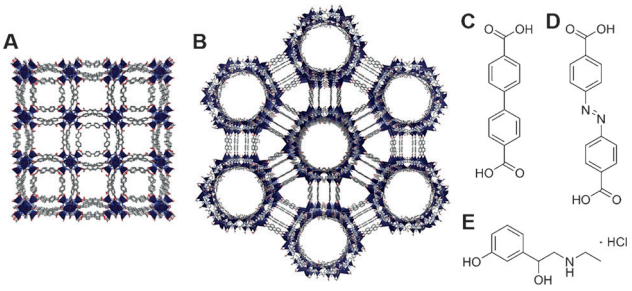

Figure 1. Structure of A) bMOF-1 and B) bMOF-100, C) BPDC, D) Azo-BPDC, and E) etilefrine hydrochloride (Zn^{2+}, dark blue; C, dark gray; N, blue; O, red; H omitted for clarity).

[a] *H. Oh, Prof. J. An*
Department of Chemistry Education
Seoul National University
1 Gwanak-ro, Gwanak-gu
Seoul 151-748 (Republic of Korea)
E-mail: jihyunan@snu.ac.kr

[b] *Dr. T. Li*
Department of Chemistry
University of Pittsburgh
219 Parkman Avenue, Pittsburgh
Pennsylvania 15260 (USA)

Supporting information for this article is available on the WWW under http://dx.doi.org/10.1002/chem.201501560.

Etilefrine hydrochloride (Figure 1 E) was chosen as the target drug molecule for delivery and release. Etilefrine is an alpha-adrenergic agonist and has been used to prevent syncopal recurrence and priapism.[27] It is a cardiac stimulant that is commonly employed as an antihypotensive for the treatment of orthostatic hypotension.[28] Etilefrine hydrochloride shows cationic properties when dissolved in solution; therefore, it was expected to exhibit excellent loading properties in the negatively charged bMOFs through cation exchange.

Results and Discussion

We examined whether the chosen crystalline bMOFs would maintain their crystallinity and morphology after soaking in Nanopure water and SBF by PXRD and SEM. The PXRD patterns in Nanopure water (37 °C) showed that the long-range crystallinities of bMOF-1 and bMOF-4 were maintained up to approximately 50 days, whereas the crystallinities of bMOF-100 and bMOF-102 were lost within 1 day (see the Supporting Information, Figure S1). The SEM image of bMOF-1 in water showed that both the shape and surface of the material suffered a small amount of damage after 80 days. It was shown that neither the shape nor the surface of bMOF-4 were maintained as well as those of bMOF-1 after 50 days in water. Neither bMOF-100 nor bMOF-102 maintained their original crystalline shape (Figure S3 in the Supporting Information). The stability of all bMOFs was also monitored in SBF (at 37 °C, pH 7.40). The PXRD data showed that both bMOF-1 and bMOF-4 appeared to maintain their crystallinity up to approximately 40 and 35 days, respectively (Figure S2 in the Supporting Information). The SEM images of bMOF-100 and bMOF-102 in SBF were not significantly different from those in Nanopure water. The SEM images of bMOF-1 and bMOF-4 in SBF show that the surfaces of these materials were also damaged, and they appeared rough after 80 and 50 days in SBF, respectively (Figure S4 in the Supporting Information).

We then explored how the structure and stability of the material influenced the drug release profile. bMOF-1 and bMOF-4 have structures containing a microporous 1D channel, whereas bMOF-100 and bMOF-102 have structures containing a mesoporous 3D pore. All of these bMOFs are anionic and contain dimethyl ammonium (DMA) cations to balance the charge of the frameworks. Thus, etilefrine hydrochloride was loaded into the micro-sized bMOFs through the use of a cation exchange process. The completion of drug loading was monitored by ^{1}H NMR spectroscopic analysis; the amount of cation-exchanged drug was evaluated from the spectra by analyzing the stoichiometric ratio of cationic drugs versus the anionic sites (see the Supporting Information). The time needed to complete etilefrine hydrochloride loading in bMOF-100 and bMOF-102 (1 day) was shorter than that of bMOF-1 and bMOF-4 (2 days). This is attributed to the greater accessibility of mesoporous bMOF-100 and bMOF-102 because of the larger window size as well as because of the interconnected 3D pore geometry.

The amount of drug loaded into bMOF-1 and bMOF-4 was 0.110 ± 0.007 g and 0.113 ± 0.006 g per 1 g of materials, respectively; bMOF-100 and bMOF-102 contained 0.106 ± 0.0085 g and 0.122 ± 0.009 g of drug, respectively, per 1 g of materials. The negative charge of each framework per unit is compensated by two DMA cations; therefore, two etilefrine per framework were expected to be encapsulated through cation exchange. Molar ratios of drugs versus frameworks were 2.18 and 2.24 per $Zn_8(ad)_4(ligand)_6O$ for bMOF-1 and bMOF-4, respectively, whereas bMOF-100 and bMOF-102 had molar ratios of 2.02 and 2.39 per $Zn_8(ad)_4(ligand)_6(OH)_2$, respectively. Interestingly, the amount of drug in the mesoporous MOFs (pore volume ca. 4.3 $cm^3 g^{-1}$) was similar to those of the microporous MOFs (pore volume ca. 0.75 $cm^3 g^{-1}$) in spite of their larger pore volume. These materials only contain the minimum amount of cations to balance the frameworks. No excess drug was found in the pore.

Simulated body fluid (SBF) was used as an artificial biological environment. The experiment was also run in Nanopure water to determine the efficacy of the cation exchange process with this particular cationic drug. The temperature was maintained at 37 °C. All samples were analyzed by high-performance liquid chromatography (HPLC).

During the first two days, rapid drug release from all bMOFs was observed (Figure 2). Subsequently, drug release slowed down dramatically, for the most part, until the entire amount of loaded drug was released into SBF. The time needed for complete release from the material was 80 days in the case of bMOF-1, 49 days for bMOF-4, 69 days for bMOF-100, and 54 days for bMOF-102. Completion of release was determined by ^{1}H NMR spectroscopic analysis, which confirmed that no remaining drug was present in the materials (see the Supporting Information).

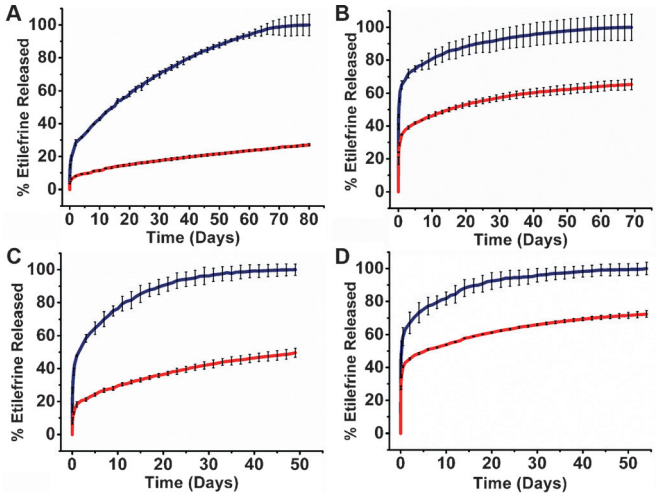

Figure 2. Percentage of drug released over time (in days) for each material in SBF (blue) and Nanopure water (red). A) bMOF-1, B) bMOF-100, C) bMOF-4, and D) bMOF-102.

The long period of release of bMOFs is quite unusual; most reports on drug release from micro-sized MOFs in biological buffered solution completed within 1–3 weeks under a wide range of circumstances and conditions. Although a simple

comparison of these studies is difficult, such a profound difference in time frames is notable. bMOF-1, in particular, was shown to have a unique and exciting drug-release profile. In this case, it took 15 days before half of the drug was released from bMOF-1 into SBF, 26 days before 65% release was achieved, 41 days before 80% and 80 days until completion. The drug-release data from bMOF-1 in SBF lent itself nicely to a model wherein three segmented linear plots describe the curve with accuracy (Figure S21 in the Supporting Information). Specifically, from 2 to 23 days the rate of release was 1.63% per day, from 24 to 44 days the rate was 1.00% per day, and from 45 to 64 days the rate was 0.64% per day. This clearly shows that bMOF-1 exhibits remarkable time-release properties with respect to etilefrine hydrochloride. bMOF-4 also exhibited time release of the drug, although not as steadily as, or over the extended timeframe of bMOF-1, but at a much more uniform rate than shown by bMOF-100 and bMOF-102 during the early stages of drug release. BMOF-4 released half of the contained drug into SBF within two days, 65% after five days, and 80% after 12 days. Following the period of rapid release over the first three days, the release profile of bMOF-4 exhibited discrete phases through which it showed consistent drug release rates; 2.47% per day from 3 to 12 days, and 0.95% per day from 15 to 24 days. bMOF-100 and bMOF-102, however, released half of the loaded drug after only 4 h, and 65% after 1 and 1.5 days, respectively, and 80% after 10 and 8.5 days, respectively (Table 1). Clearly, none of these release profiles approach the time release potential of bMOF-1, but on a smaller scale bMOF-4 differentiates itself from bMOF-100 and bMOF-102 by settling into relatively slow and steady release rates after the abrupt release of about half of the drug (2 days). bMOF-100 and bMOF-102 released nearly 63–65% within one day. After the rapid release at the beginning of the experiment, however, bMOF-100 and bMOF-102 were slow to release the remainder of the drug, hovering near the asymptote longer than bMOF-4. In these cases, the last 10% of the drug, which remained in bMOF-100 and bMOF-102, was released over a period of 47 and 38 days, respectively, with a release rate averaging 0.21 and 0.26% per day. bMOF-4 finished releasing completely after 49 days, whereas bMOF-100 and bMOF-102 completed at 69 and 54 days, respectively. This hovering phenomenon is probably due to a very slow release of the trapped drug in the collapsed MOFs.

Table 1. Amount of loaded drug and drug release of bMOFs in SBF.

	bMOF-1	bMOF-4	bMOF-100	bMOF-102
Max load [$g/g_{materials}$] NMR[a] (HPLC[b])	0.110 (0.111)	0.113 (0.109)	0.106 (0.105)	0.122 (0.127)
50% release[c]	15 days	1.5 days	4 h	4 h
65% release[c]	26 days	5 days	1 day	1.5 days
80% release[c]	41 days	12 days	10 days	8.5 days
100% release[c]	80 days	49 days	69 days	54 days

[a] Based on NMR spectroscopic analysis. [b] Based on HPLC analysis. [c] In SBF at 37 °C.

The bMOFs released the drug at different rates in Nanopure water, suggesting that cation exchange may contribute to the release of the cationic drug. Approximately 27.1% of the drug was released from bMOF-1 into Nanopure water at the completion of the experiment in SBF. bMOF-4, bMOF-100, and bMOF-102 had released about 49.6, 65.3, and 72.5%, respectively, of the drug in Nanopure water after completion of their respective experiments in SBF. The experiments for bMOF-1 and bMOF-4 in Nanopure water produced markedly different curves compared with those obtained in the respective SBF experiments, which underlines the effectiveness of the cation transfer process in these cases. bMOF-100 and bMOF-102, however, showed minimal differentiation in Nanopure water from their respective experiments in SBF. Not only were the values similar, but they also seemed to follow a similar curve to the SBF experiments. It is likely that the cation exchange process had a minimal impact upon the abilities of bMOF-100 and bMOF-102 to release etilefrine hydrochloride because of their rapid structural degradation. bMOF-1 showed the most significant deviation from the experiment in Nanopure water. The drastically different rates of release suggest that the cation exchange process had a profound effect in this case.

The structural stability of the bMOFs in SBF and Nanopure water was analyzed subsequent to release through SEM imaging of as-synthesized materials, drug-loaded materials, and materials after the completion of the drug release experiments (Figure 3). SEM images of bMOFs after drug loading for four days show that some bMOF crystals became slightly less-faceted compared with the as-synthesized bMOFs. This shows that some of the bMOFs might have experienced partial degradation during the drug-loading process. Upon completion of drug release in SBF, some preserved bMOF-1 and bMOF-4 were found in SEM images. Although the surface of these materials seems to be highly damaged, part of the crystalline structures of bMOF-1 and bMOF-4 maintained their shape after drug release. However, bMOF-100 and bMOF-102 did not retain their structure after complete drug release and crystals were not found in the SEM images. On the other hand, when etilefrine hydrochloride was released in Nanopure water, the materials experienced some degradation during the experiment, but to a lesser extent than the damage sustained by the materials after releasing in SBF. We also observed by SEM that some bMOF-100 and bMOF-102 remained after release in Nanopure water (Figure S20 in the Supporting Information).

Powder X-ray diffraction (PXRD) patterns were obtained from the as-synthesized materials, drug-loaded materials, and materials after the conclusion of the drug-release experiments in SBF and in Nanopure water (Figure 4). After drug loading, all materials were shown to have their crystallinity preserved when compared with the as-synthesized materials. bMOF-1 and bMOF-4 were also shown to have retained some of their crystallinity after the drug had been completely released. On the other hand, there were no PXRD patterns found from bMOF-100 and bMOF-102 subsequent to the drug-release ex-

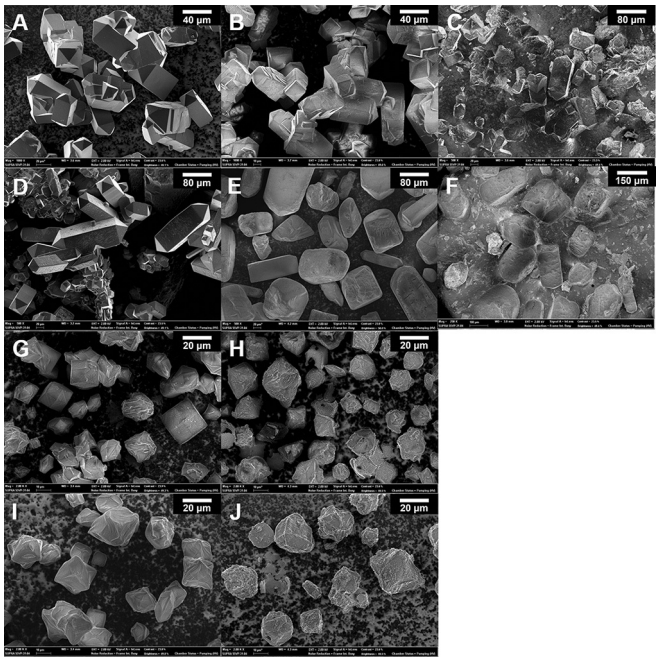

Figure 3. SEM images of bMOFs. Columns from left: A) as-synthesized, B) after drug loading, C) after releasing in SBF. Rows from top: A) bMOF-1, D) bMOF-4, G) bMOF-100, I) bMOF-102. Scale bars: A, B = 40 μm, C–E = 80 μm, F = 150 μm, G–J = 20 μm.

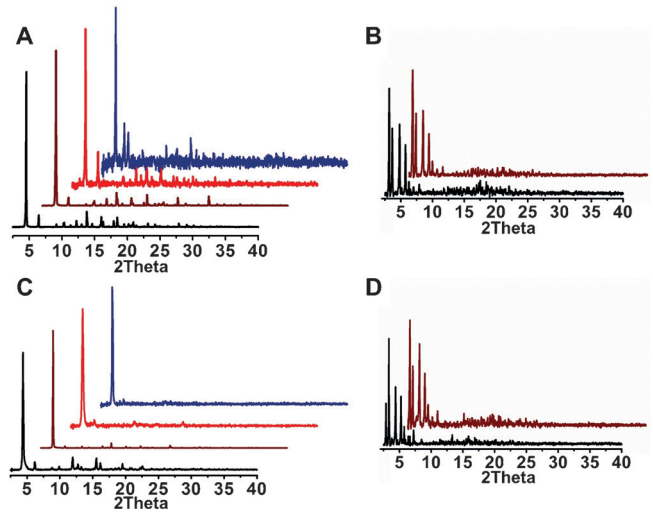

Figure 4. PXRD patterns of bMOFs. A) bMOF-1, B) bMOF-100, C) bMOF-4, and D) bMOF-102 (as synthesized, black; after drug loading, brown; after releasing in NP water, red; after releasing in SBF, blue).

periments in either SBF or Nanopure water, and the crystallinity of the structure seems to be completely lost. In the cases of bMOF-1 and bMOF-4, PXRD patterns were obtained throughout the release process. The PXRD patterns of bMOF-1 showed that the loss of crystallinity became clearer after eight weeks of release study in SBF. The PXRD patterns of bMOF-4 were shown to have a peak shift after seven weeks of release study in SBF (Figures S22 and S23 in the Supporting Information).

To gain a better understanding of the structural stability of bMOFs during the process of drug release, the amount of

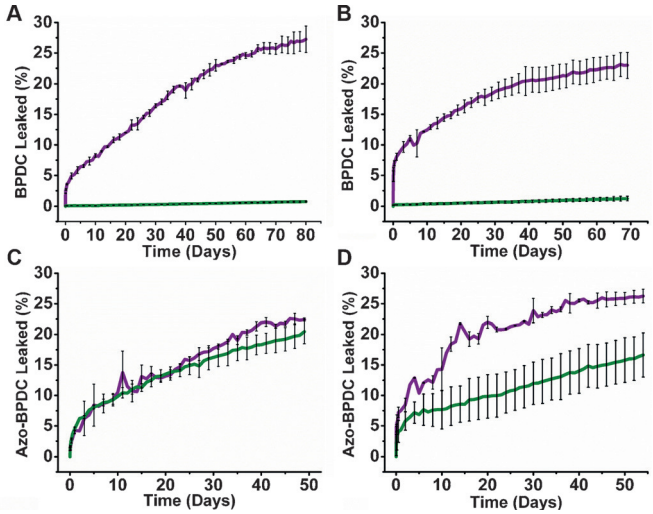

Figure 5. Percentage of ligand released over time (in days) for each material in SBF (purple) and Nanopure water (green). A) bMOF-1 (BPDC), B) bMOF-100 (BPDC), C) bMOF-4 (Azo-BPDC), and D) bMOF-102 (Azo-BPDC).

ligand leached from the frameworks was measured simultaneously with the amount of drug released (Figure 5). The amount of ligand in each sample was analyzed concurrently by HPLC to monitor the degradation of each MOF over time. In the cases of bMOF-1 and bMOF-100, the amount of BPDC released into the solution of Nanopure water at completion was 0.76 and 1.25% of the BPDC composing the materials, respectively, but the amount of BPDC released from the materials in SBF was approximately 27.2 and 23.0% of the ligand comprising them, respectively. bMOF-4 and bMOF-102 showed slightly different trends. bMOF-4 and bMOF-102 released approximately 20.5 and 16.7% of the Azo-BPDC in Nanopure water, respectively, and 22.5 and 26.6% in SBF, respectively. The results show that the ligands dissociated from materials in SBF at a higher rate than those from materials in Nanopure water, as was expected due to the active biological environment. They also show that the Azo-BPDC ligand dissociates from the materials at a much greater rate than BPDC in Nanopure water. At the beginning of the process in SBF, bMOF-100 and bMOF-102 showed an almost doubled percentage of ligand leakage compared with those of bMOF-1 and bMOF-4. The data collected for the calculation of the amount of the leaked ligand clearly does not provide a direct correlation with the stability of the materials.

Stability studies of bMOFs during and after release experiments suggest that the materials either partially or completely degrade during the release process. This structural degradation certainly leads to some of the drug being released into the solution. The release profile could be influenced by the degree of degradation. A burst of most of the drug release of bMOF-100 and bMOF-102 at the beginning of the process can be explained by immediate structural degradation of bMOF-100 and bMOF-102. As a consequence of the rapid structural collapse of bMOF-100 and bMOF-102, drug release seems to be mainly administrated through structural degradation with minimal impact from cation exchange. The unusual release profile of

bMOF-1 is probably attributed to slower degradation of material in the buffered solution. It is possible, in this case, for bMOF-1 to be heavily influenced by the cation exchange process because the structure is sufficiently robust to withstand cation exchange before sustaining significant levels of degradation. bMOF-4, being less stable than bMOF-1, but much more stable than bMOF-100 and bMOF-102, had its drug release considerably influenced by both degradation and cation exchange. Ultimately, the mechanism of drug release of bMOFs is not completely understood; however, our study suggests that both bMOF degradation and cation exchange between the cations in SBF and the loaded drug may contribute as factors in drug release of bMOFs.

Conclusion

The use of bMOFs as delivery materials was studied using etilefrine hydrochloride as the drug molecule to be delivered through a cation exchange process. After drug loading, which was accomplished by soaking the bMOFs into a solution of etilefrine hydrochloride in ethanol, the drug was released into SBF until completion. During this time, the amount of ligand released by the bMOFs was closely monitored in addition to the amount of drug released. All of the studied bMOFs showed an initial burst release, followed by a steady reduction in release rate until completion. The incorporated drug was released over a time period ranging from 49 to 80 days. These seem to be unique characteristics of these bMOFs and clearly they all warrant further study. Among these, however, bMOF-1 was undoubtedly the standout. After the initial burst release, bMOF-1 settled into a slow and remarkably steady release pattern. This is quite a surprising result and would seem to lend itself well to sustained release formulations, although further study is needed to determine whether this is a function of the interaction of the small molecule etilefrine hydrochloride with bMOF-1 or whether it is an intrinsic property of bMOF-1. It was also fairly stable under experimental conditions, even to the point of retaining a portion of its crystalline structure after delivering its entire payload, which may have contributed to the slow and consistent rate of release. We fully expect to see bMOFs continue to make their presence known in the area of drug delivery, whether that is for targeted delivery, sustained release formulations, or both.

Experimental Section

General procedures and protocols

Unless otherwise mentioned, all chemicals were purchased from Sigma-Aldrich; *N*,*N*′-dimethylformamide (DMF) and Azobenzene-4,4′-dicarboxylic acid (Azo-BPDC) were purchased from Samchun Chemical and Tokyo Chemical Industry Co., respectively. Dimethylsulfoxide-d_6 ([D_6]DMSO) was purchased from Cambridge Isotope Laboratory, Inc. DMF was pre-dried with molecular sieves overnight before use; other purchased chemicals were used directly without further purification. Powder X-ray diffraction (PXRD) patterns were collected with a Bruker New D8 Advance powder diffractometer equipped with a $Cu_{K\alpha}$ X-ray source at 40 kV, 40 mA with a scan speed of 0.20 s per step and a step size of 0.02°. ^{1}H NMR spectra were recorded with a JEOL JNM-LA400 spectrometer with LFG (400 MHz). All ^{1}H NMR data are reported in ppm (δ) downfield from [D_6]DMSO. Field emission scanning electron microscopy (FESEM) images were taken with a SUPRA 55VP field emission scanning electron microscope. Fourier transform infrared (FTIR) spectra were collected with a PerkinElmer Spectrum 2000 Explorer FTIR spectrometer and KBr pellet samples. Absorptions are described as follows: very strong (vs), strong (s), medium (m), weak (w), shoulder (sh), and broad (br). Elemental microanalysis was performed with a Flash EA 1112 by the Stable Isotope Laboratory, National Instrumentation Center for Environmental Management at Seoul National University. Nanopure water (18.2 mΩ) was collected with a ELGA purelab option Q. Thermogravimetric analysis (TGA) was performed with a TA Q50 thermal analysis system. All TGA experiments were run under a N_2 atmosphere from 25–600 °C at a rate of 10 °C min^{-1}.

MOF synthesis

bMOF-1: Each stock solution of adenine (0.05 M, 0.125 mmol), zinc acetate dihydrate (0.05 M, 0.375 mmol), biphenyl-4,4′-dicarboxylic acid (BPDC) (0.1 M, 0.25 mmol), and nitric acid (1 M, 1 mmol) was prepared in DMF and added to a 20 mL vial. Nanopure water (1.5 mL) was added to the vial and heated at 130 °C for 24 h. The crystals were collected and washed with DMF.

bMOF-4: Each stock solution of adenine (0.05 M, 0.015 mmol), zinc acetate dihydrate (0.05 M, 0.045 mmol), and Azo-BPDC (0.1 M, 0.03 mmol) was prepared in DMF and mixed well in a Pyrex tube. Nanopure water (0.1 mL) was then added to the tube. After freezing in liquid nitrogen, the Pyrex tube was placed under vacuum (200 mTorr) and sealed. The sealed tube was heated at 130 °C for 24 h. The crystals were collected and washed with DMF and ethanol. The crystals were dried under N_2 gas (15 min) for further analysis. Yield: 9.6 mg (70.4% based on adenine); FTIR (KBr 4000–400 cm^{-1}): $\tilde{\nu}$ = 3420 (br), 3121 (br), 2968 (w), 1604 (s), 1561 (s), 1475 (m), 1393 (s), 1384 (s), 1290 (w), 1213 (m), 1153 (m), 1094 (m), 1010 (m), 869 (m), 790 (s), 705 (m), 640 (m) cm^{-1}; elemental analysis calcd (%) for $C_{127.5}H_{158.5}N_{40.5}O_{48}Zn_8 = Zn_8(ad)_4(Azo\text{-}BPDC)_6O{\cdot}2(NH_2(CH_3)_2)^+$, 16.5 H_2O, 6.5 DMF: C 43.14, H 4.50, N 15.98; found C 43.47, H 4.29, N 15.03.

bMOF-100: Each stock solution of adenine (0.05 M, 0.125 mmol), zinc acetate dihydrate (0.05 M, 0.25 mmol), and BPDC (0.1 M, 0.25 mmol) was added to a 20 mL vial. DMF (2.5 mL), methanol (1 mL), and Nanopure water (0.25 mL) were then added to the vial and heated at 85 °C for 24 h. The crystals were collected and washed with DMF.

bMOF-102: A stock solution of Azo-BPDC (4 mL, 0.05 M) in DMF was added to a 20 mL vial containing pre-synthesized bMOF-100 crystals (220 mg). The vial was heated at 85 °C for 24 h, then cooled to RT. The crystals were washed with DMF (2×4 mL) and fresh Azo-BPDC solution (4 mL, 0.05 M) in DMF was added. The vial was then heated at 85 °C for 24 h. The crystals were collected and washed with DMF.

Drug loading: Etilefrine hydrochloride loading was performed by cation exchange. Etilefrine hydrochloride was purchased from Tokyo Chemical Industry, Co., and used without further purification. A solution of etilefrine hydrochloride in absolute ethanol (0.1 M) was prepared. The as-synthesized bMOFs were soaked in etilefrine hydrochloride solution for 15 min, then the solvent was removed. The bMOFs were again soaked in fresh etilefrine hydrochloride solution for 15 min and the solvent was again removed (2×). The

bMOFs were soaked again in fresh etilefrine hydrochloride solution, and the solution was replaced every 12 h for 4 days.

Quantitative NMR: Drug loading calculations: To determine the amount of drug loaded on each bMOF, ^{1}H NMR spectra were collected. NMR samples were prepared by digesting drug-loaded bMOFs in [D_6]DMSO (0.7 mL) with deuterium chloride solution (35 wt.% in D_2O, 0.3 μL). 1,3,5-Trioxane (6.5 mg) was added to the NMR sample as an internal standard for quantification of the drug. The amount of drug loaded was calculated by comparing the ^{1}H NMR peak ratio of 1,3,5-trioxane and the drug (see the Supporting Information).

SBF preparation: Simulated body fluid (SBF) was prepared as follows.[29] Nanopure water (200 mL) was added to a 250 mL plastic beaker with a stirring bar and heated to 36.5±1.5 °C. The following chemicals were added sequentially, maintaining the temperature at 36.5±1.5 °C: sodium chloride (2.009 g), sodium bicarbonate (0.088 g), potassium chloride (0.0562 g), potassium phosphate dibasic trihydrate (0.0575 g), magnesium chloride hexahydrate (0.0778 g), hydrochloric acid solution in H_2O (10 mL, 1.0 M), calcium chloride (0.0732 g), and sodium sulfate (0.018 g). With the insertion of an electrode of a pH meter in the solution, Nanopure water was added up to 225 mL in total. Tris(hydroxymethyl) aminomethane (TRIS) (1.5158 g) was slowly added until the pH reached 7.45± 0.01, then 1.0 M HCl solution was added to lower the pH to 7.42± 0.01. When all TRIS was added, the final temperature and pH of the solution were adjusted with 1.0 M HCl solution to 36.5 °C and pH 7.40.

High-performance liquid chromatography (HPLC): Reverse-phase HPLC was performed at ambient temperature with an Agilent 1220 Infinity liquid chromatographic system equipped with diode array and a variable wavelength detector using a Poroshell 120 column (4.6 mm×100 mm) with a flow rate of 0.089 mL min^{-1}. The mobile phase consisted of 0.4% formic acid (v/v) in a mixture of acetonitrile and water (37:63). The effluent was monitored at 274 nm to identify the maximum absorbance peak of etilefrine hydrochloride separate from that of formic acid (see the Supporting Information).

Drug release in SBF: The appropriate dried etilefrine-loaded bMOF (20 mg) was added to a 4 mL vial (diameter 1.2 cm). SBF (1 mL, pH 7.40) was added to the vial and kept at 37 °C. At defined times, an aliquot of solution (150 μL) was taken from the vial and fresh SBF (150 μL) was added to the vial. The solution taken from the vial was analyzed by HPLC to measure the concentration of etilefrine in the solution. This was repeated for each bMOF.

Drug release in Nanopure water: The appropriate dried etilefrine-loaded bMOF (20 mg) was added to a 4 mL vial. Nanopure water (1 mL, 18.2 mΩ) was added to the vial at 37 °C. At defined times, an aliquot of solution (150 μL) was used for each measurement and fresh Nanopure water (150 μL) was added to the vial. The solution taken from the vial was analyzed by HPLC to measure the concentration of etilefrine in the solution. This was repeated for each bMOF.

Acknowledgements

This work was supported by the Aspiring Researcher Program through Seoul National University Research (SNU) in 2013. The authors acknowledge the assistance of Professor Nathaniel L. Rosi from the University of Pittsburgh.

Keywords: cations · drug delivery · kinetics · medicinal chemistry · metal–organic framework

[1] G. Férey, *Chem. Soc. Rev.* **2008**, *37*, 191 – 214.
[2] J. R. Long, O. M. Yaghi, *Chem. Soc. Rev.* **2009**, *38*, 1213 – 1214.
[3] A. C. McKinlay, R. E. Morris, P. Horcajada, G. Ferey, R. Gref, P. Couvreur, C. Serre, *Angew. Chem. Int. Ed.* **2010**, *49*, 6260 – 6266; *Angew. Chem.* **2010**, *122*, 6400 – 6406.
[4] I. Imaz, M. Rubio-Martinez, J. An, I. Sole-Font, N. L. Rosi, D. Maspoch, *Chem. Commun.* **2011**, *47*, 7287 – 7302.
[5] J. An, O. K. Farha, J. T. Hupp, E. Pohl, J. I. Yeh, N. L. Rosi, *Nat. Commun.* **2012**, *3*, 604.
[6] H. Xu, J. Cai, S. Xiang, Z. Zhang, C. Wu, X. Rao, Y. Cui, Y. Yang, R. Krishna, B. Chen, G. Qian, *J. Mater. Chem. A* **2013**, *1*, 9916 – 9921.
[7] J. An, S. J. Geib, N. L. Rosi, *J. Am. Chem. Soc.* **2009**, *131*, 8376 – 8377.
[8] J. An, C. M. Shade, D. A. Chengelis-Czegan, S. Petoud, N. L. Rosi, *J. Am. Chem. Soc.* **2011**, *133*, 1220 – 1223.
[9] T. M. Allen, P. R. Cullis, *Science* **2004**, *303*, 1818 – 1822.
[10] G. Tiwari, R. Tiwari, B. Sriwastawa, L. Bhati, S. Pandey, P. Pandey, S. K. Bannerjee, *Int. J. Pharm. Investig.* **2012**, *2*, 2 – 11.
[11] R. Langer, *Nature* **1998**, *392*, 5 – 10.
[12] J. R. Brouwers, *Pharm. World Sci.* **1996**, *18*, 153 – 162.
[13] P. Horcajada, C. Serre, G. Maurin, N. A. Ramsahye, F. Balas, M. Vallet-Regi, M. Sebban, F. Taulelle, G. Ferey, *J. Am. Chem. Soc.* **2008**, *130*, 6774 – 6780.
[14] P. Horcajada, T. Chalati, C. Serre, B. Gillet, C. Sebrie, T. Baati, J. F. Eubank, D. Heurtaux, P. Clayette, C. Kreuz, J. S. Chang, Y. K. Hwang, V. Marsaud, P. N. Bories, L. Cynober, S. Gil, G. Ferey, P. Couvreur, R. Gref, *Nat. Mater.* **2010**, *9*, 172 – 178.
[15] A. C. McKinlay, B. Xiao, D. S. Wragg, P. S. Wheatley, I. L. Megson, R. E. Morris, *J. Am. Chem. Soc.* **2008**, *130*, 10440 – 10444.
[16] I. Imaz, M. Rubio-Martinez, L. Garcia-Fernandez, F. Garcia, D. Ruiz-Molina, J. Hernando, V. Puntes, D. Maspoch, *Chem. Commun.* **2010**, *46*, 4737 – 4739.
[17] F. Ke, Y. P. Yuan, L. G. Qiu, Y. H. Shen, A. J. Xie, J. F. Zhu, X. Y. Tian, L. D. Zhang, *J. Mater. Chem.* **2011**, *21*, 3843 – 3848.
[18] M. R. di Nunzio, V. Agostoni, B. Cohen, R. Gref, A. Douhal, *J. Med. Chem.* **2014**, *57*, 411 – 420.
[19] N. Liédana, P. Lozano, A. Galve, C. Tellez, J. Coronas, *J. Mater. Chem. B* **2014**, *2*, 1144 – 1151.
[20] C. He, K. Lu, D. Liu, W. Lin, *J. Am. Chem. Soc.* **2014**, *136*, 5181 – 5184.
[21] C. Y. Sun, C. Qin, C. G. Wang, Z. M. Su, S. Wang, X. L. Wang, G. S. Yang, K. Z. Shao, Y. Q. Lan, E. B. Wang, *Adv. Mater.* **2011**, *23*, 5629 – 5632.
[22] D. Cunha, M. Ben Yahia, S. Hall, S. R. Miller, H. Chevreau, E. Elkaim, G. Maurin, P. Horcajada, C. Serre, *Chem. Mater.* **2013**, *25*, 2767 – 2776.
[23] J. S. Qin, D. Y. Du, W. L. Li, J. P. Zhang, S. L. Li, Z. M. Su, X. L. Wang, Q. Xu, K. Z. Shao, Y. Q. Lan, *Chem. Sci.* **2012**, *3*, 2114 – 2118.
[24] H. N. Wang, X. Meng, G. S. Yang, X. L. Wang, K. Z. Shao, Z. M. Su, C. G. Wang, *Chem. Commun.* **2011**, *47*, 7128 – 7130.
[25] S. R. Miller, D. Heurtaux, T. Baati, P. Horcajada, J. M. Greneche, C. Serre, *Chem. Commun.* **2010**, *46*, 4526 – 4528.
[26] T. Li, M. T. Kozlowski, E. A. Doud, M. N. Blakely, N. L. Rosi, *J. Am. Chem. Soc.* **2013**, *135*, 11688 – 11691.
[27] A. Raviele, M. Brignole, R. Sutton, P. Alboni, P. Giani, C. Menozzi, A. Moya, *Circulation* **1999**, *99*, 1452 – 1457.
[28] E. Miller, L. Wiener, D. Bloomfield, *Arch. Neurol.* **1973**, *29*, 99 – 103.
[29] A. Oyane, H. M. Kim, T. Furuya, T. Kokubo, T. Miyazaki, T. Nakamura, *J. Biomed. Mater. Res. Part A* **2003**, *65*, 188 – 195.

Received: April 22, 2015
Published online on September 25, 2015